OPTIMAL-FEEDBACK ACCELERATED PICARD ITERATION METHODS AND A FISH-SCALE GROWING METHOD FOR WIDE-RANGING AND MULTIPLE-REVOLUTION PERTURBED LAMBERT'S PROBLEMS

Xuechuan Wang,* Satya N. Atluri†

Wide-ranging and multiple-revolution perturbed Lambert's problems are building blocks for practical missions such as development of cislunar space, interplanetary navigation, orbital rendezvous, etc. However, it is of a great challenge to solve these problems both accurately and efficiently, considering the long transfer time and the complexity of high-fidelity modeling of space environment. For that, a methodology combining Optimal-Feedback Accelerated Picard Iteration methods and Fish-Scale Growing Method is demonstrated. The resulting iterative formulae are explicitly derived and applied to restricted three-body problems and multi-revolution earth rendezvous problem. The examples demonstrate the validity and high efficiency of the proposed methods.

INTRODUCTION

The Lambert's problem has been studied extensively in literature. However, when perturbations and long transfer time are taken into account, this problem could still be very challenging for the most state-of-art algorithms of orbital design. The challenge comes from two aspects. First, the various perturbation factors in a high-fidelity model of orbital mechanics lead to extremely complex expressions of nonlinear terms and large-scale computations. Further, as the transfer time is prolonged, the terminal state of the orbit becomes very sensitive to the initial state and thus it could be very difficult to find a good initial approximation of the transfer orbit. To overcome these difficulties, it requires that the algorithms should possess the following merits: large convergence area, high approximating accuracy, low computational complexity, and ease of parallel processing.

Mathematically, the Lambert's problem can be described as a two-point boundary value problem to be solved via various numerical methods involving the shooting methods [1, 2, 3] and collocation methods. Specifically, collocation method [4] plays an important role in solving various Lambert's problems in relative orbit transfer [5], optimal control of spacecraft formation flying [6], low-thruster transfer between earth and moon [7], etc. In the conventional collocation method, however, one needs to construct nonlinear algebraic equations and calculate the inverse of the Jacobian matrix, which could be very troublesome. Some simpler ideas without inverting matrices are introduced by the modified Chebyshev-Picard iteration (MCPI) method proposed by Junkins et al. [8], and the Optimal-Feedback Accelerated Picard Iteration (OFAPI) methods by Wang and Atluri [9,10,11].

* Research Assistant, Department of Mechanical Engineering, Texas Tech University, Lubbock, Texas, 79415.
† Presidential Chair & University Distinguished Professor, Department of Mechanical Engineering, Texas Tech University, Lubbock, Texas, 79415.

Further, directly solving a Lambert's problem with long duration time and perturbations is often impossible due to the limited convergence area of the algorithms and the sensitivity of initial guess. For that, the so-called Fish-Scales-Growing Method (FSGM) [9] is used in this paper. In a conservative system, the solution of a two-point boundary value problem is determined by the principle of least action. It allows us to breakdown a Lambert's problem with long transfer time into several smaller time intervals using the Fish-Scales-Growing Method. Moreover, the orbit transfer problems defined in each sub-interval can be solved independently, thus the proposed algorithm can be conveniently coded for parallel computation to enhance the computational efficiency. Theoretically, in a conservative system the present Fish-Scales-Growing Method will converge to the true solution for any arbitrary initial approximation, as long as the orbit transfer problem in each sub-interval can be solved.

Overall, the aim of this paper is to propose a new solving algorithm of Lambert's problem that manages to ensure the convergence of long-range transfer even in chaotic systems, and also achieve very high computational accuracy and efficiency even when dealing with extremely complex perturbation model. Several orbit transfer problems in the Earth-Moon and Sun-Earth three body systems, as well as a multi-revolution earth orbit rendezvous problem will be used as examples to validate the proposed algorithm. All these problems are of long transfer time, sensitive to computational error, and difficult to converge for shooting methods and common collocation methods.

The structure of this paper is as following. In the methodology part, we briefly introduced the Optimal-Feedback Accelerated Picard Iteration method and the Fish-Scales-Growing Method. The formulae and flowchart of these two methods are provided explicitly. In the part of problem description, the dynamical models of restricted three body problem and multi-revolution Earth orbit problem are presented along with the system parameters. Then, in the part of simulation results, we validated the proposed methods by solving several orbit transfer problems related with deep-space exploration and multi-revolution rendezvous. Some conclusions are reached at the end.

METHODOLOGY

The Optimal-Feedback Accelerated Picard Iteration (OFAPI) Method

Generally, for solving a system of first order differential equations

$$\dot{\mathbf{x}} = \mathbf{g}(\mathbf{x}, \tau)\,,\ \tau \in \left[t_0, t\right], \tag{1}$$

the OFAPI method approximates the solution at any time t with an initial approximation $\mathbf{x}_0(\tau)$ and the correctional iterative formula as

$$\mathbf{x}_{n+1}(t) = \mathbf{x}_n(\tau)\big|_{\tau=t} + \int_{t_0}^{t} \boldsymbol{\lambda}(\tau)\{\dot{\mathbf{x}}_n(\tau) - \mathbf{g}[\mathbf{x}_n(\tau), \tau]\}d\tau\,, \tag{2}$$

where $\boldsymbol{\lambda}(\tau)$ is a matrix of Lagrange multipliers yet to be determined. Eq. (2) indicates that the $(n+1)$ th correction to the analytical solution $\mathbf{x}_{n+1}$ involves the addition of $\mathbf{x}_n$ and a feedback weighted optimal error in the solution $\mathbf{x}_n$ up to the current time t . $\boldsymbol{\lambda}(\tau)$ can be optimally determined by making the right-hand side of Eq. (2) stationary about $\delta\mathbf{x}_n(\tau)$, thus resulting the constraints.

$$\begin{cases} \delta\mathbf{x}_n(\tau)\big|_{\tau=t} : \mathbf{I} + \boldsymbol{\lambda}(\tau)\big|_{\tau=t} = \mathbf{0} \\ \delta\mathbf{x}_n(\tau) : \dot{\boldsymbol{\lambda}}(\tau) + \boldsymbol{\lambda}(\tau)\mathbf{J}(\tau) = \mathbf{0} \end{cases},\ t_0 \le \tau \le t\,, \tag{3}$$

where $\mathbf{J}(\tau) = \partial \mathbf{g}(\mathbf{x}_n, \tau) / \partial \mathbf{x}_n$.

First order Taylor series approximation of $\boldsymbol{\lambda}(\tau)$ can be readily obtained from the Eq. (3), in the following form

$$\boldsymbol{\lambda}(\tau) \approx \mathbf{T}_0[\boldsymbol{\lambda}] + \mathbf{T}_1[\boldsymbol{\lambda}](\tau - t) , \tag{4}$$

where $\mathbf{T}_k[\boldsymbol{\lambda}]$ is the k th order differential transformation of $\boldsymbol{\lambda}(\tau)$, i.e.

$$\mathbf{T}_k[\boldsymbol{\lambda}] = \frac{1}{k!} \frac{d^k \boldsymbol{\lambda}(\tau)\big|_{\tau=t}}{d\tau^k} . \tag{5}$$

Using Eq. (3), $\mathbf{T}_k[\boldsymbol{\lambda}]$ can be determined in an iterative way:

$$\mathbf{T}_0[\boldsymbol{\lambda}] = diag[-1,-1,...] , \ \mathbf{T}_{k+1}[\boldsymbol{\lambda}] = -\frac{\mathbf{T}_k[\boldsymbol{\lambda}\mathbf{J}]}{k+1} , \ 0 \le k \le K+1 . \tag{6}$$

Let $\mathbf{G} = \dot{\mathbf{x}}_n(\tau) - \mathbf{g}[\mathbf{x}_n(\tau), \tau]$, by substituting Eq. (6) into Eq. (2), we have

$$\mathbf{x}_{n+1}(t) = \mathbf{x}_n(t) + \int_{t_0}^{t} \{\mathbf{T}_0[\boldsymbol{\lambda}] + \mathbf{T}_1[\boldsymbol{\lambda}](\tau - t)\}\mathbf{G} d\tau , \tag{7}$$

Two other ways of approximating $\boldsymbol{\lambda}(\tau)$ have been proposed by the authors leading to 3 distinct OFAPI algorithms [11].

Suppose $\mathbf{x}(t)$ is approximated by a vector of trial functions $\mathbf{u}$. Let each element u_e of the trial function be the linear combinations of basis functions $\phi_{e,nb}(t)$

$$u_e = \sum_{nb=1}^{N} \alpha_{e,nb} \phi_{e,nb}(t) = \boldsymbol{\Phi}_e(t) \mathbf{A}_e . \tag{8}$$

Through collocating points in time domain, from Eq. (7) we have

$$\mathbf{U}_{n+1} = \mathbf{U}_n + (\tilde{\mathbf{T}}_0 - [\tilde{\mathbf{T}}_1 \cdot \tilde{\mathbf{t}}]) \tilde{\mathbf{E}} \tilde{\mathbf{G}} + \tilde{\mathbf{T}}_1 \tilde{\mathbf{E}} [\tilde{\mathbf{t}} \cdot \tilde{\mathbf{G}}] , \tag{9}$$

which can be used to iteratively solve for the values of $\mathbf{x}(t)$ at collocated time points. For higher computational efficiency and accuracy, we set the basis functions as orthogonal polynomials. Herein, the first kind of Chebyshev polynomials are adopted, and the collocation points in each time interval are selected as Chebyshev-Gauss-Lobatto (CGL) nodes. For further details of Eq. (9) please refer to [10].

A flow chart of OFAPI method is provided herein

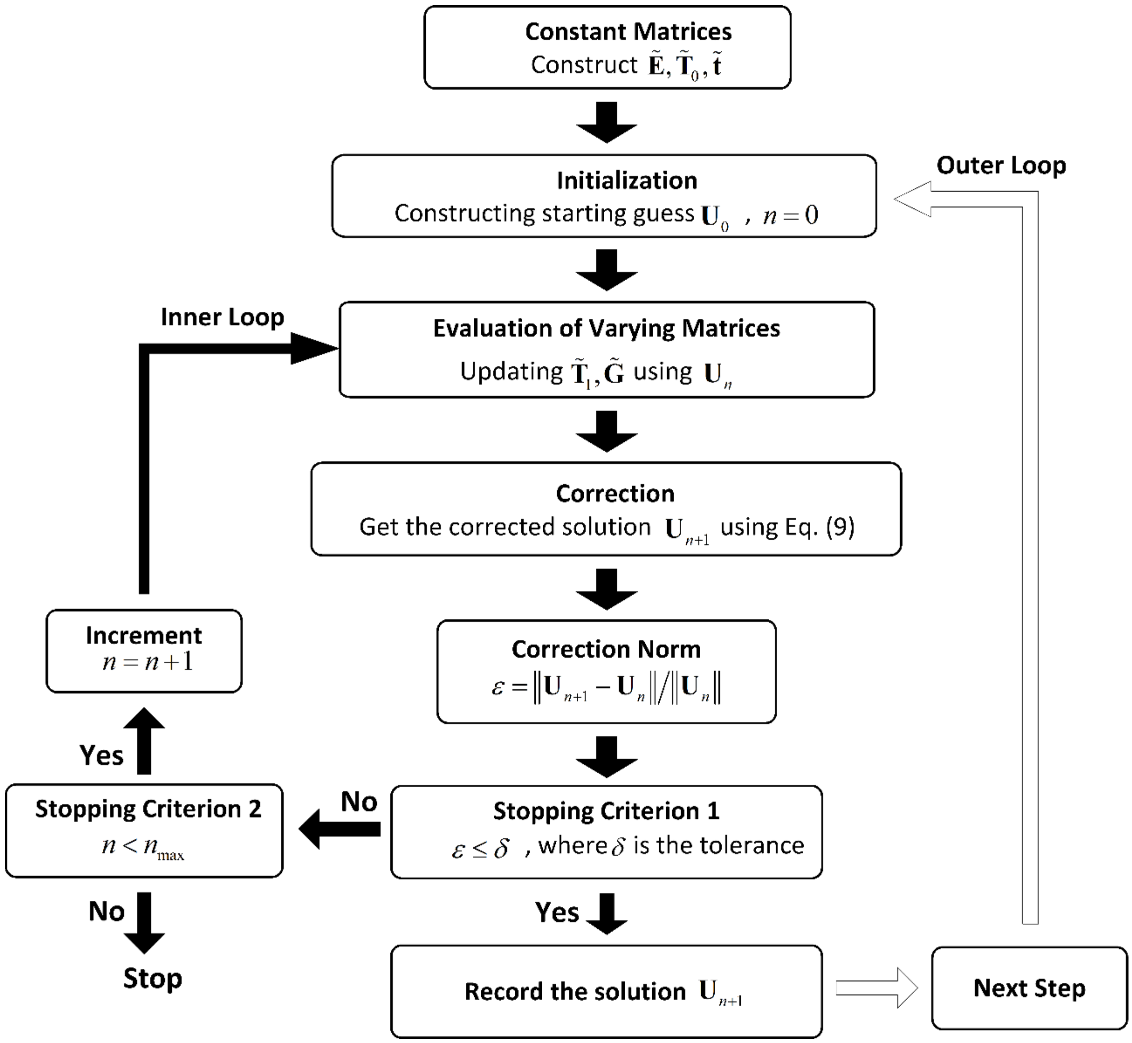

Figure 1 The flow chart of OFAPI method for solving nonlinear differential equations

The Fish Scales Growing Method

The iterative procedure of this method is as follows. An initial approximation is provided by a reference trajectory, which could be a nominal solution obtained from the linearized problem or unperturbed problem. Then divide the domain (t_0, t_f) of the two-point boundary value problem (TPBVP) into multiple isometric intervals $[t_i, t_{i+1}]$, $0 \le i < N$, $t_{i+1} - t_i = (t_f - t_0)/N$. For each interval, the points $\mathbf{x}(t_i)$ and $\mathbf{x}(t_{i+1})$ on the reference trajectory are set as boundaries. In each iteration, we need to solve the N TPBVPs defined by the boundaries $\mathbf{x}(t_i)$ and $\mathbf{x}(t_{i+1})$ in the corresponding interval $[t_i, t_{i+1}]$. The points $\tilde{\mathbf{x}}(t_j)$, $t_j = (t_i + t_{i+1})/2$ on the solutions of these $N+1$ TPBVPs are collected for the next step. Then we solve the $N-1$ TPBVPs defined by the boundaries $\tilde{\mathbf{x}}(t_j)$ and $\tilde{\mathbf{x}}(t_{j+1})$, $0 \le j < N-1$ in the corresponding interval $[t_j, t_{j+1}]$. After that, the points $\bar{\mathbf{x}}(t_i)$ on the solutions of these $N-1$ TPBVPs are used to replace $\mathbf{x}(t_i)$ and $\mathbf{x}(t_{i+1})$. If

$\left\|\bar{\mathbf{x}}(t_i)-\mathbf{x}(t_i)\right\| \le \varepsilon$, the iteration ends. Otherwise one should replace $\mathbf{x}(t_i)$ with $\bar{\mathbf{x}}(t_i)$ and restart the iteration.

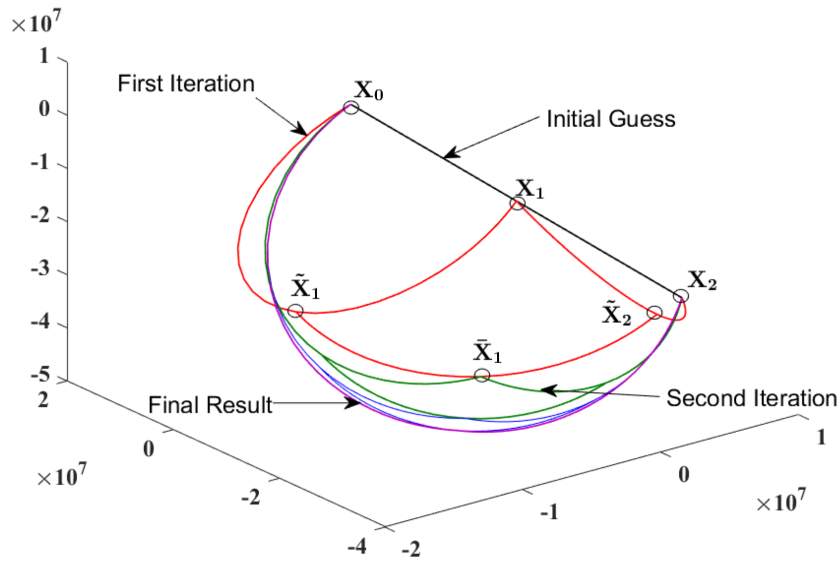

Figure 2 Illustration of the FSGM

A schematic of the Fish-Scales-Growing Method is illustrated in Fig. 2. The domain $[t_0, t_f]$ is divided into two smaller intervals $[t_0, t_1]$ and $[t_1, t_f]$, where $t_1 = (t_0 + t_f)/2$. In each iteration, three boundary value problems are defined and need to be solved so as to correct the position values $\mathbf{x}_1$ at the time instant t_1. As the iteration goes on, $\mathbf{x}_1$ approaches to the real value, thus the piecewise trajectory evolves to the true solution of the original TPBVP. A flow chart of this method is provided in Fig. 3.

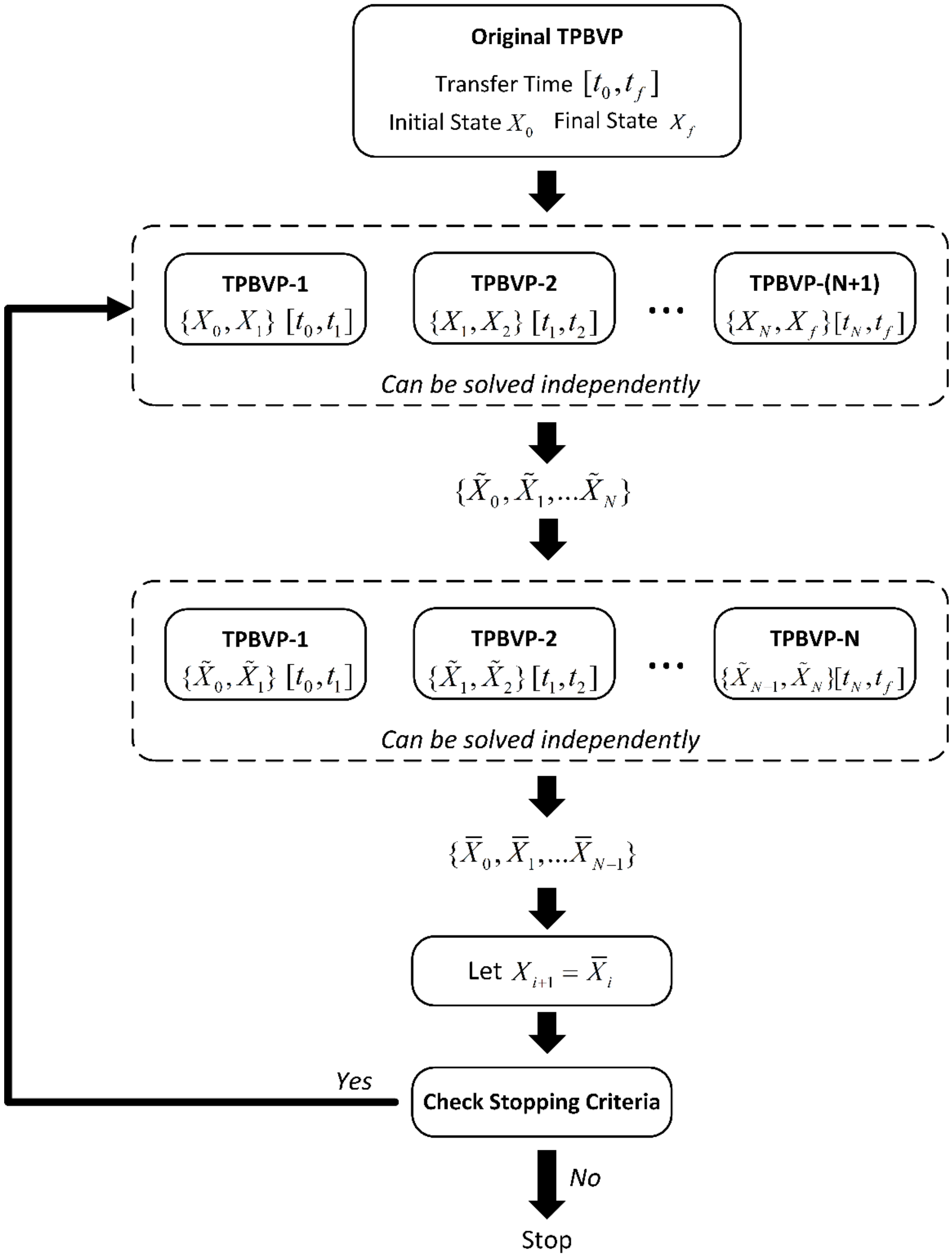

Figure 3 Flowchart of FSGM

PROBLEM DESCRIPTION

In the previous work [9], the potential of OFAPI method was revealed by solving the orbital propagation problem and the earth orbit transfer within one revolution, in conjunction with FSGM, where it is shown to have better performance than the conventional MCPI method. Herein, a computational scheme is proposed to extend these methods to solve practical orbit transfer problems in much larger space and time scales.

Orbit Transfer in Three Body System

The circular restricted three-body problem (CR3BP) in the Earth-Moon system is used to formulate the dynamics herein. Denoting the primary body (Earth), the secondary body (Moon), and the third body (Spacecraft) as P1, P2, P3 respectively, the motion of P3 is governed by the following dimensionless equations.

$$\begin{gathered}\ddot{x}-2\dot{y}-x=-\frac{(1-\mu)(x+\mu)}{d^3}-\frac{\mu}{r^3}(x-1+\mu)\\ \ddot{y}+2\dot{x}-y=-\frac{(1-\mu)}{d^3}y-\frac{\mu}{r^3}y \qquad (10)\\ \ddot{z}=-\frac{(1-\mu)}{d^3}z-\frac{\mu}{r^3}z\end{gathered}$$

where $d=\sqrt{(x+\mu)^2+y^2+z^2}$, $r=\sqrt{(x-1+\mu)^2+y^2+z^2}$ are distances from P3 to P1 and P2 respectively. The mass fraction is $\mu=m_2/(m_1+m_2)$, where m_1 and m_2 are masses of P1 and P2 respectively. The positions and velocities compose the state vector $[x,y,z,\dot{x},\dot{y},\dot{z}]$.

Note that the Earth-Moon orbit transfer procedure is usually composed of two stages. The first stage is cataloging and choosing an unstable manifold in space that departures Earth and fly to Moon. It could be an orbit around the libration point, or an unstable resonant orbit. The second stage is determining a transfer orbit from a certain point on the manifold and the final Moon orbit. Herein, we are interested in the second stage where the transfer orbit is calculated. The parameters for Earth-Moon system and Sun-Earth system are provided in Table 1.

Table 1. Parameters of three body systems

	Distance	Mass Fraction	Period	Non-dimensional Position of L_1
Earth-Moon	384400 km	0.012277471	30 days	[0.8363,0,0]
Sun-Earth	149597870 km	3.0542e-06	365 days	[0.99,0,0]

Multi-revolution Earth Orbit Transfer

The dynamical model of an Earth orbit can be simply described by

$$\ddot{\mathbf{r}}=-\frac{\mu}{r^3}\mathbf{r}+\mathbf{a}_p\,, \qquad (11)$$

where μ is the gravitational parameters, $\mathbf{r}=[x,y,z]^T$ is the position vector in the inertial frame, $r=\sqrt{x^2+y^2+z^2}$, and $\mathbf{a}_p$ is the perturbation acceleration.

Although the governing equations take a simple form herein, it can become extremely complex as full gravity force of Earth and other perturbations are included. Moreover, for a multi-revolution problem, the maximum number of revolutions is

$$N_{\max} = floor(\frac{\Delta t}{2\pi}\sqrt{\frac{\mu}{a_m^3}}), \tag{12}$$

where Δt is the transfer time and a_m is related with the initial and final positions. In that case, the number of possible transfer orbits are $2N_{\max}+1$. In this paper, a high-fidelity model incorporating higher order gravity force will be considered to examine the proposed computational scheme.

SIMULATION RESULTS

Direct Transfer between Earth and Low Moon Orbit

Using the dimensionless model of CR3BP. An Earth-Moon orbit transfer problem is solved using the OFAPI method in conjunction with the present Fish-Scales-Growing Method. Figure 4 shows an example of direct transfer from 185-km Earth orbit to 100-km Lunar orbit. Using Fish-Scale Growing Method (FSGM), the transfer problem is broken down into several subproblems, which are then solved independently using OFAPI method. Fig. 4 (a) demonstrates the intriguing evolution of the piecewise solution from a straight line (initial guess) to an accurate transfer orbit (final solution). Using the initial velocity provided by the final solution of OFAPI-FSGM scheme, the ode113 (MATLAB) is initialized and generates a testing orbit shown in Fig. 4 (b). The comparison between the final solution of OFAPI-FSGM and the testing orbit shows that they match very well. Note that ode113 itself cannot solve boundary value problems, herein it is just used to integrate the orbit trajectory with the initial condition provided by the proposed scheme. As is aforementioned, the FSGM is not bothered by the selection of initial guess, because it is absolutely and globally convergent in conservative systems. This statement is verified by the results presented in Fig. 4.

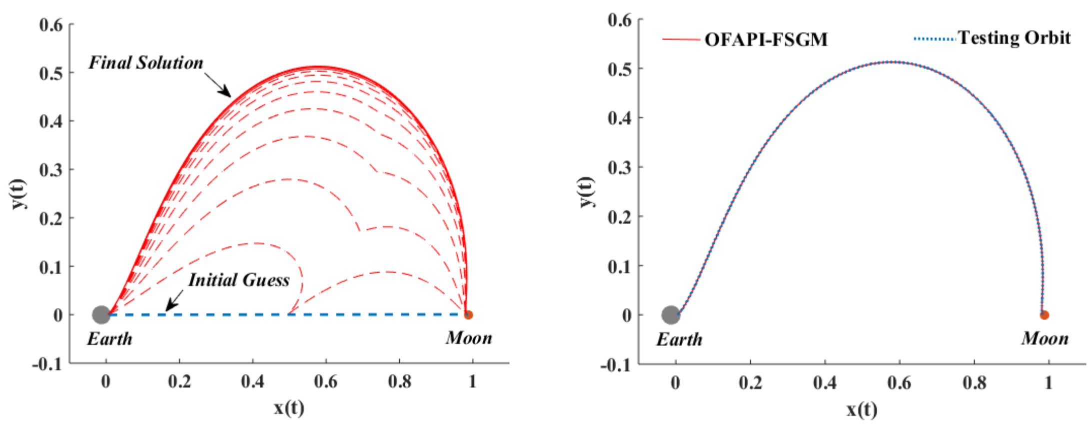

(a) (b)

Figure 4 Earth to Moon transfer orbit obtained using OFAPI-FSGM

The parameters of this orbit transfer problem and the configurations of the proposed methods are listed in Table 2, where L denotes the number of segments in this orbit transfer, and N denotes the number of collocation points used in each segment.

Table 2. List of parameters in the Earth to Moon orbit transfer problem

Problem Parameters			Method Configuration	
Initial State	Final State	Transfer Time	N	L

0.0171-u	1-u-0.0048	0.54π	201	2
0	0	(8 days)		
0	0			

Since the final solution is composed of two segments of trajectories, there is a discontinuity of velocity at the meeting node. Denoting the abrupt change of velocity as δv , it decreases monotonically to a very small value through the correction of trajectories using FSGM. The iterative correction process of FSGM is recorded in Fig. 5 (a). By comparing with the integrating results of ode113 (its precision has been set to the highest), the computational error of the final solution is recorded in Fig. 5 (b).

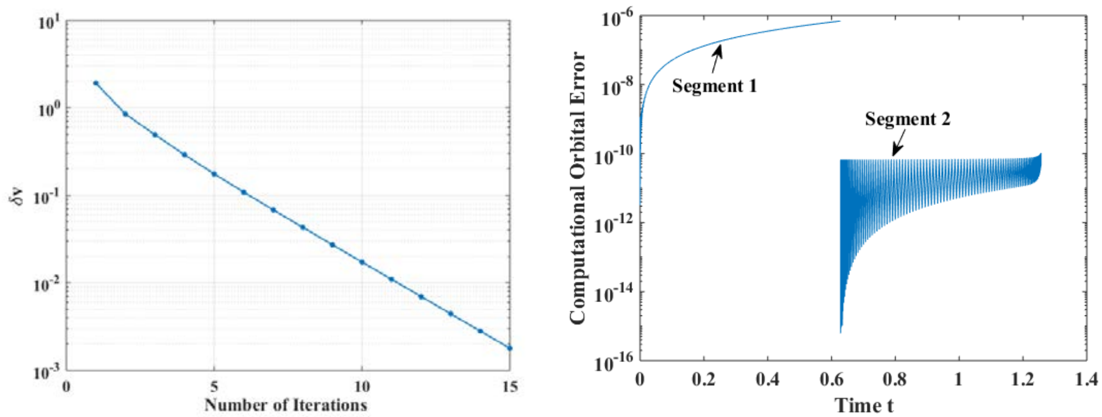

(a) (b)

Figure 5 (a) Change of velocity discontinuity (δv) at meeting node. (b) Computational error of the orbital position.

As is shown in Fig. 5, the final solution obtained by FAPI-FSGM is very smooth and highly accurate. Compared with other methods for orbital transfer between Earth and Moon, taking shooting method for instance, the proposed method is very straightforward and easy to use, because no refined initial guess is needed and the convergence is much more guaranteed. Using the same initial guess in Fig 4, the normal shooting method will diverge immediately.

Direct Transfer between Earth and Moon Halo Orbit

The direct transfer between Earth and Moon halo orbit is often accomplished with the aid of stable and unstable manifolds of halo orbits. Take the orbit transfer from Earth to Moon L_1 Halo orbit for example, the transfer consists of two legs. One is from Earth parking orbit to the stable manifold, and the other is flying along the manifold without or with little energy cost. Since the stable manifold can be obtained by simply propagating backward from the halo orbit, most effort is spent on seeking the transfer from Earth to the manifold. For that, conventional approach needs to select a tentative transfer orbit first, either by experience or by Monte Carlo test. Then the shooting method is used to refine the tentative orbit by differential-correction. However, the searching process could be time consuming and inconvenient to use when arbitrarily boundary conditions and transfer time are specified. An alternative way using OFAPI-FSGM is introduced herein to find the transfer orbit from an Earth orbit to the stable manifold, where the initial condition, the final condition, and the transfer time are arbitrarily selected. An example is provided to demonstrate the proposed method. The simulation results are presented in Fig. 6.

The parameters of this orbit transfer problem and the configurations of the proposed methods are listed in Table 3.

Table 3. List of parameters in the Earth to Moon halo orbit transfer problem

Problem Parameters			Method Configuration	
Initial State (Earth orbit)	Final State (Stable manifold)	Transfer Time (Earth to stable manifold)	N	L
0.0171-u	0.02934	0.2π	71	3
0	0.3579	(3 days)		
0	0			

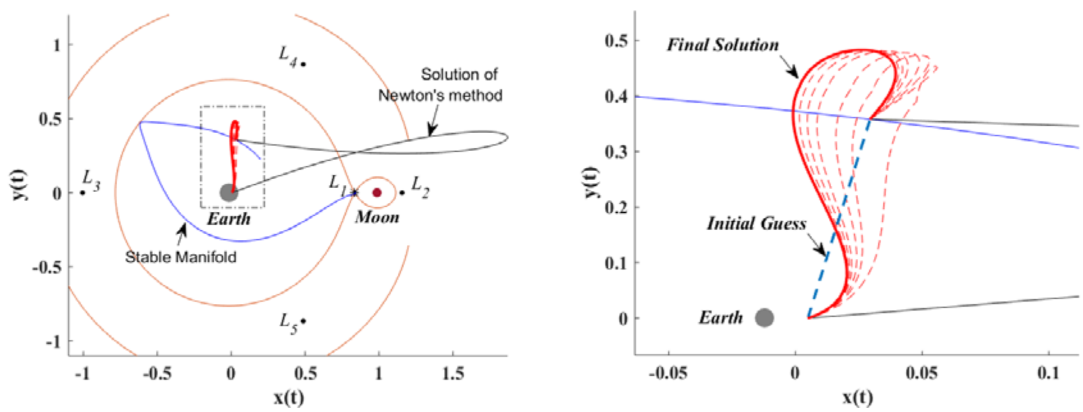

(a) (b)

Figure 6 Earth to Moon halo orbit transfer using OFAPI- FSGM

Similarly to the previous example, a straight line linking the initial state and final state is used to kick-start the OFAPI-FSGM. Note that in this example the transfer orbit is divided into three segments instead of two. During the iteratively correcting process of OFAPI-FSGM, the changes of velocity discontinuities (δv_1 and δv_2) at the meeting nodes are recorded in Fig. 7. It is shown that the velocity discontinuities between the neighboring segments decrease monotonically and quickly converges to nearly zero. The computational accuracy of the OFAPI-FSGM is also relatively very high, and can be further improved by refine the solution using more nodes in each segment.

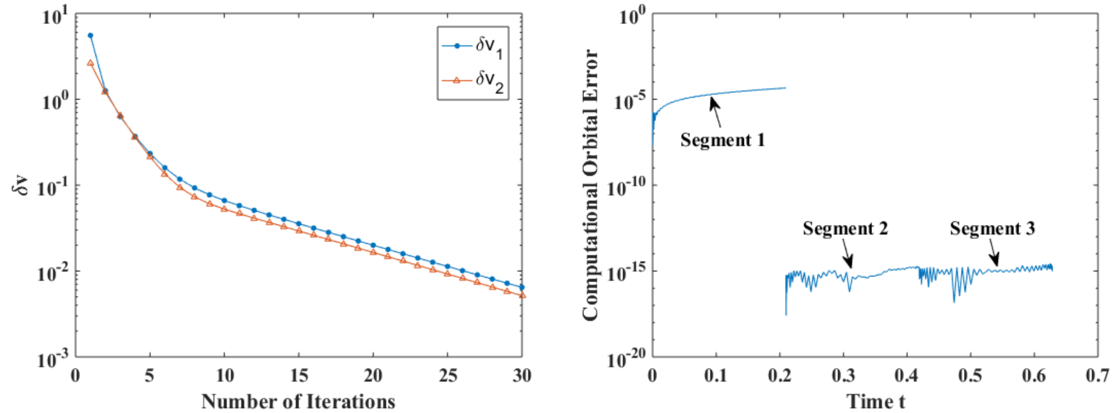

(a) (b)

Figure 7 (a) Change of velocity discontinuity (δv) at meeting node. (b) Computational error of the orbital position.

From the obtained transfer orbit, the departing velocity is $v_0 = [6.0334, 8.6513, 0]$, and the arrival velocity at the inserting point is $v_f = [-0.1992, -1.1372, 0]$. The velocity of the stable manifold is $v_{sm} = [-1.3848, 0.727, 0]$ at the inserting point. All the values are obtained in the rotating coordinates of CRTBP. By using the same initial guess in Fig. 6, the Newton based collocation method converges to another transfer orbit by chance, as indicated with the black line in Fig. 6. However, this transfer orbit is obviously undesirable.

Low Energy Transfer between Earth and Earth Halo Orbit

In the previous example, the stable manifold of Moon halo orbit does not encounter Earth. Thus, a bridge is needed to transfer from Earth to the halo orbit. However, this is not the case in Sun-Earth system. It is well known that the stable manifold of Earth L_1 halo orbit passes Earth, which provides much more convenience on designing the transfer orbit. In this example, we use a roughly integrated stable manifold of halo orbit at the vicinity of Earth to kick-start the OFAPI-FSGM. Herein, OFAPI is not directly used to solve boundary value problems, but instead as a highly efficient numerical integrator and incorporated into shooting method, i.e., each segment of the transfer orbit in Fig. 8 is obtained by OFAPI-Shooting.

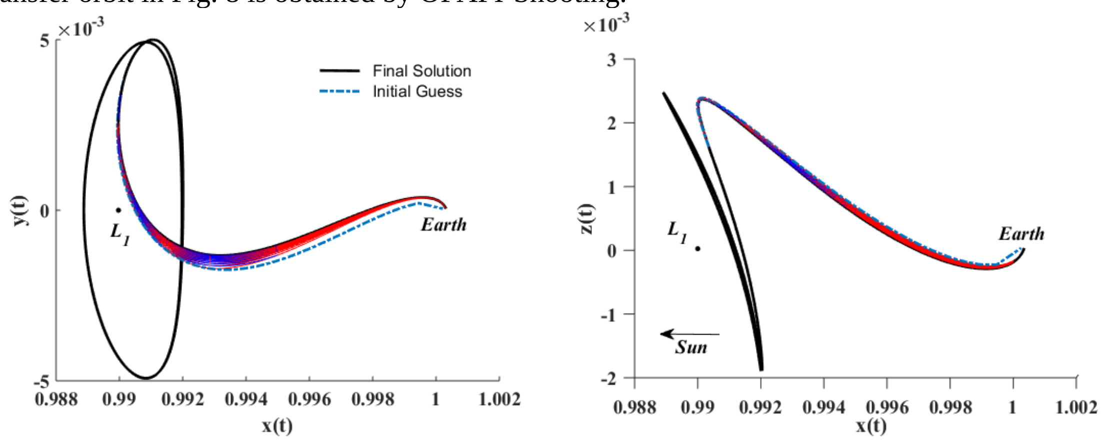

(a) (b)

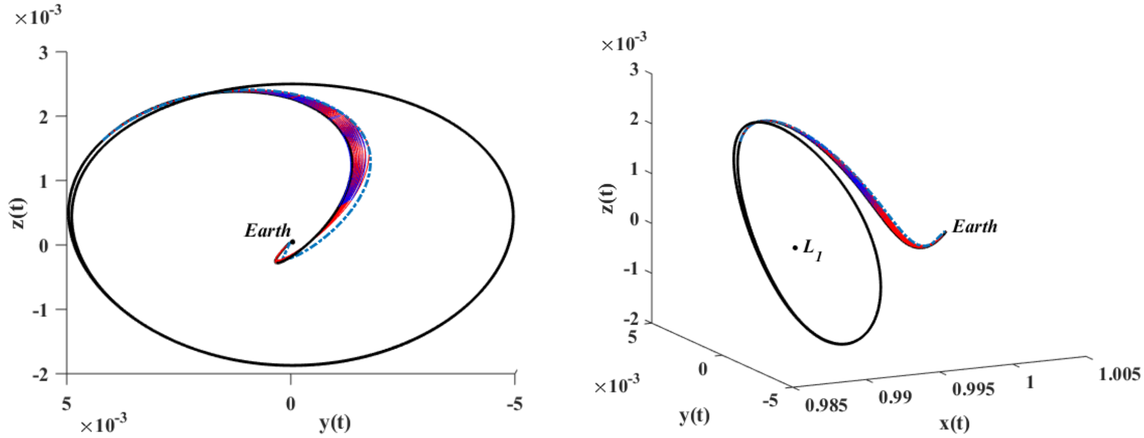

(c) (d)

Figure 8 Earth to Earth halo orbit transfer using OFAPI-FSGM

The parameters of this orbit transfer problem and the configurations of the proposed methods are listed in Table 4.

Table 4. List of parameters in the Earth to Earth halo orbit transfer problem

Problem Parameters			Method Configuration		
Initial State	Final State	Transfer Time	N	K	L
0.99034	1.0003	2.084	21	20	4
0.00434	4.369e-5	(116days)			
0.00150	1.058e-5				

The iteratively correcting process using FAPI-FSGM is recorded in Fig. 9. As shown, the trajectory is obviously non-smooth in the first iteration, due to the discontinuity of velocity at the meeting nodes. However, this discontinuity is significantly eased up in the following iterations. It is worth to note that is hard to integrate accurately the stable manifold of the L_1 Earth halo orbit, because of its chaotic nature in the Sun-Earth three body system. By using ode113 integrator of MATLAB, we found that even at its highest accuracy, the numerical integration along the stable manifold still have observable divergence. For that reason, it is very difficult for common shooting methods to accurately determine the transfer orbit in this case.

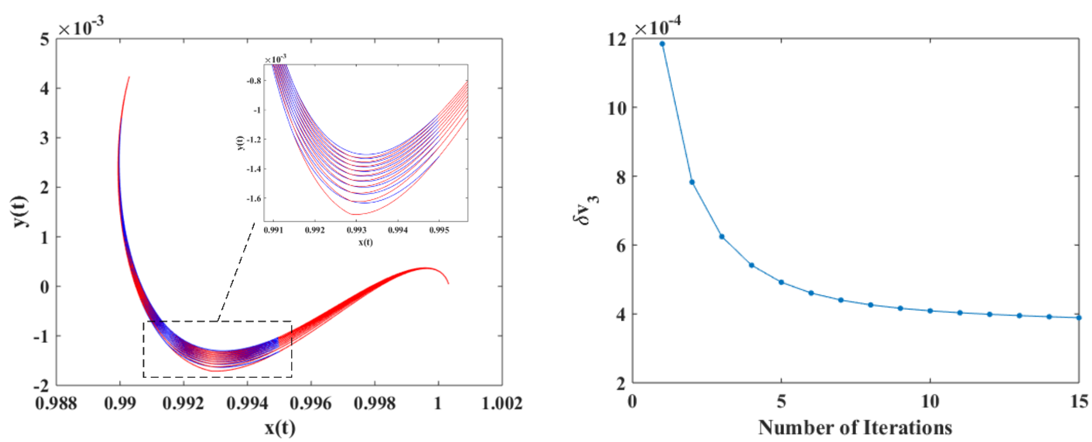

(a) (b)

Figure 9 (a) Iteratively correcting process of the transfer orbit. (b) Change of velocity discontinuity (δv) at meeting node.

Multi-revolution Earth Orbit Transfer

The multi-revolution Lambert's problem is concerned in both literature and real tasks. The difficulty of solving this problem mainly lies in two aspects. One is the computational plight caused by the large amount of perturbation terms in full gravity model of Earth. The other one is the sensitivity of final state to initial state due to the long transfer time, which may cause computational inaccuracy and failure of convergence to common shooting method. To some extent, the proposed methods, FAPI and FSGM, can overcome these two difficulties. In a previous paper [9], it is shown that the OFAPI method magnificently reduces the computational burden of evaluating the perturbation terms of gravity force, in comparison with high-order Runge-Kutta method. Moreover, the FSGM allows the division of a long transfer duration into several shorter segments that the common shooting methods can deal with.

Herein, a multi-revolution problem with the transfer time being $[0s, 360{,}000s]$, approximately 4 days, is solved by OFAPI-Shooting method in conjunction with FSGM, where the transfer is divided into two segments. Each segment is further divided into 10 intervals to convenience the numerical integration using OFAPI. In each segment the solution is approximated using 13 collocation points. The parameters of this orbit transfer problem and the configurations of the proposed methods are listed in Table 5.

The Keplerian orbit is used as an initial approximation for the multi-revolution orbit transfer. As shown in Fig. 10, the transfer orbit obtained in the first iteration is obviously non-smooth, indicating large discrepancy from the true solution. To evaluate the improvement of the solution obtained using the proposed method, the discrepancy δv of the velocity at the meeting node of the two segments is recorded and plotted in Fig. 11. It is shown that the proposed method further improves the Keplerian solution and the discrepancies decrease monotonically.

Table 5. List of parameters in the multi-revolution Earth orbit transfer problem

Problem Parameters			Method Configuration		
Initial State (m)	Final State (m)	Transfer Time (s)	N	K	L
4.2164172e7	3.573110e7	360,000	10	13	2
0	2.2375813e7	(4 days)			
0	0				

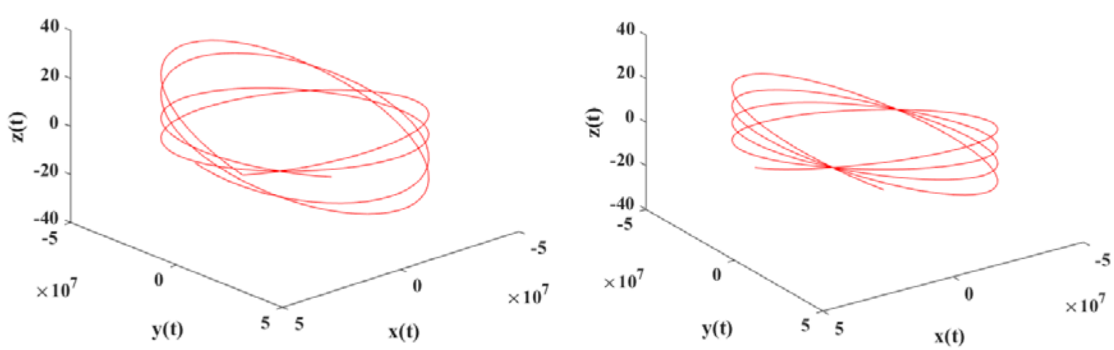

(a) (b)

Figure 10 Test of FSGM in multi-revolution lambert’s problem

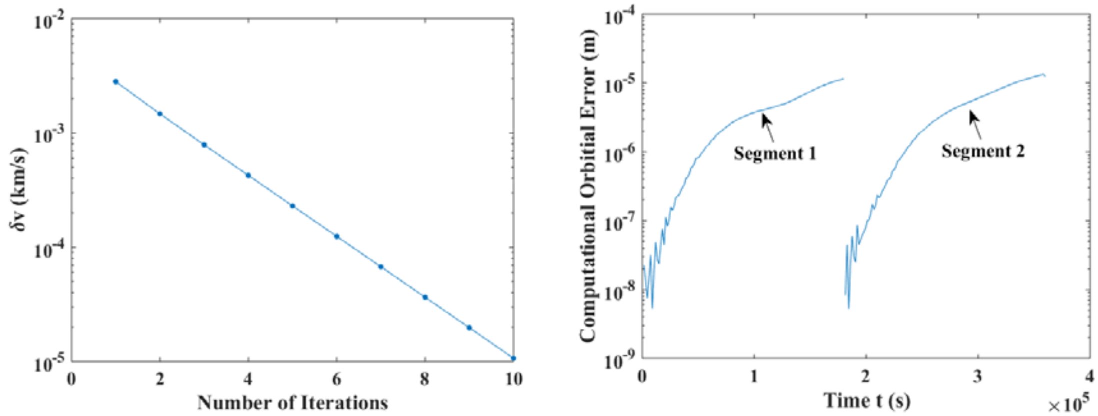

(a) (b)

Figure 11 (a) Change of velocity discontinuity (δv) at meeting node. (b) Computational error of the orbital position.

It is verified through this example that the proposed OFAPI-FSGM is capable of solving the multi-revolution orbit transfer problem accurately. The convergence of this algorithm is guaranteed by FSGM. According the Fig. 6 (a), it is also found that the convergence speed of the proposed method is logarithmic in the first ten iterations.

CONCLUSION

A Scheme for solving perturbed Lambert’s problem, i.e. the Optimal-Feedback Accelerated Picard Iteration (OFAPI) method in conjunction with the Fish Scales Growing Method (FSGM), is presented in this paper. This scheme enables one to break down a long-duration orbit transfer problem into many much easier subproblems and bypasses the dilemma of choosing initial approximating orbit. In the meantime, it also provides very accurate numerical solution through using the OFAPI method. Compared with the conventional MCPI method and other solvers of perturbed Lambert’s problem in literature, the proposed scheme can be applied to problems with relatively longer transfer time and still achieves high accuracy and efficiency.

This scheme is used to solve wide-ranging orbit transfer problems in three-body systems and a multiple-revolution perturbed Lambert’s problem. Simulation results demonstrate that the OFAPI-FSGM scheme is insensitive to the initial guess and converges to very accurate results. At last, since this scheme possesses the merit that the subproblems can be solved independently, much computational time can be saved using parallel processing.

REFERENCES

[1] Fox, K., “Numerical Integration of the Equations of Motion of Celestial Mechanics,” *Celestial Mechanics*, Vol. 33, No. 2, 1984, pp. 127-142.

[2] Roberts, S. M., and Shipman, J. S., *Two-Point Boundary Value Problems: Shooting Methods*, Elsevier, New York, 1972, pp. 1-231.

[3] Armellin R., Gondelach D., San Juan J. F., “Multi-revolution perturbed Lambert problem,” *2018 Space Flight Mechanics Meeting 2018*, pp. 1968.

[4] Elgohary, T. A., Junkins, J. L., Atluri, S. N., "An RBF-Collocation Algorithm for Orbit Propagation," *Advances in Astronautical Sciences: AAS/AIAA Space Flight Mechanics Meeting, 2015*.

[5] Chen, Q., Zhang, Y., Liao, S., Wan, F., "Newton-Kantorovich/Pseudospectral Solution to Perturbed Astrodynamic Two-Point Boundary-Value Problems," *Journal of Guidance, Control, and Dynamics*, Vol. 36, No. 2, 2013, pp. 485-498.

[6] Yang, Z., Luo, Y. Z., and Tang, G. J., "Homotopic Perturbed Lambert Algorithm for Long-Duration Rendezvous Optimization," *Journal of Guidance, Control, and Dynamics*, Vol. 38, No. 11, 2015, pp. 2215-2223.

[7] Pritchett R. E., Howell K. C., Grebow D. J., "Low-Thrust Transfer Design Based on Collocation Techniques: Applications in the Restricted Three-Body Problem". *AAS/AIAA Astrodynamics Specialist Conference*, 2017 Aug 21, pp. 1-20.

[8] Woollands, R. M., Younes, A. B., Junkins, J. L., "New Solutions for the Perturbed Lambert Problem Using Regularization and Picard Iteration," *Journal of Guidance, Control, and Dynamics*, Vol. 38, No. 9, 2015, pp. 1548-1562.

[9] Wang X., Yue X., Dai H., Atluri S. N., "Feedback-Accelerated Picard Iteration for Orbit Propagation and Lambert's Problem," *Journal of Guidance, Control, and Dynamics*. 2017 Jun 27;40(10):2442-51.

[10] Wang X., Pei W., Atluri S. N., "Bifurcation & chaos in nonlinear structural dynamics: Novel & highly efficient optimal-feedback accelerated Picard iteration algorithms," *Communications in Nonlinear Science and Numerical Simulation*. 2018 Dec 1; 65:54-69.

[11] Wang X., Atluri S. N., "A novel class of highly efficient and accurate time-integrators in nonlinear computational mechanics," *Computational Mechanics*. 2017 May 1;59(5):861-76.

[12] Wang X., Atluri S. N., "Computational methods for nonlinear dynamical systems," *Mechanical Engineering Reviews*. 2017;4(2):17-00040.